scientific reports

Check for updates

OPEN

Modulation of Ca^{2+} oscillation following ischemia and nicotinic acetylcholine receptors in primary cortical neurons by high-throughput analysis

Tsutomu Sasaki[1,2]✉, Sunao Hisada[1], Hideaki Kanki[1], Kazuto Nunomura[3], Bangzhong Lin[3], Kumiko Nishiyama[1], Tomohito Kawano[1], Shigenobu Matsumura[4] & Hideki Mochizuki[1]

Calcium oscillations in primary neuronal cultures and iPSCs have been employed to investigate arrhythmogenicity and epileptogenicity in drug development. Previous studies have demonstrated that Ca^{2+} influx via NMDA and nicotinic acetylcholine receptors (nAChRs) modulates Ca^{2+} oscillations. Nevertheless, there has been no comprehensive investigation into the impact of ischemia or nAChR-positive allosteric modulators (PAM) drugs on Ca^{2+} oscillations at a level that would facilitate high-throughput screening. We investigated the effects of ischemia and nAChR subtypes or nAChR PAM agonists on Ca^{2+} oscillations in high-density 2D and 3D-sphere primary neuronal cultures using 384-well plates with FDSS-7000. Ischemia for 1 and 2 h resulted in an increase in the frequency of Ca^{2+} oscillations and a decrease in their amplitude in a time-dependent manner. The NMDA and AMPA receptor inhibition significantly suppressed Ca^{2+} oscillation. Inhibition of NR2A or NR2B had the opposite effect on Ca oscillations. The potentiation of ischemia-induced Ca^{2+} oscillations was significantly inhibited by the NMDA receptor antagonist, MK-801, and the frequency of these oscillations was suppressed by the NR2B inhibitor, Ro-256981. In the 3D-neurosphere, the application of an α7nAChR agonist increased the frequency of Ca^{2+} oscillations, whereas the activation of α4β2 had no effect. The combination of nicotine and PNU-120596 (type II PAM) affected the frequency and amplitude of Ca^{2+} oscillations in a manner distinct from that of type I PAM. These systems may be useful not only for detecting epileptogenicity but also in the search for neuroprotective agents against cerebral ischemia.

Keywords Ca^{2+} oscillations, High-throughput screening, Ischemia, nAChR, PAM

Calcium (Ca^{2+}) is a crucial intracellular second messenger that precisely regulates a multitude of physiological functions within cells, particularly in the brain[1,2]. The changes in intracellular Ca^{2+} levels play a pivotal role in neurotransmitter release and other synaptic processes, as well as in regulating cell life and death[3,4]. The alterations in intracellular Ca^{2+} levels have been demonstrated to serve as a crucial biomarker for the investigation of the effects of compounds on neuronal network activity[5–7]. The occurrence of Ca^{2+} oscillations in neuronal cultures correlates with the formation of new synapses and the development of neuronal networks[8]. These oscillations correspond to bursts of network activity and can be modulated by the application of excitatory and inhibitory compounds[9]. The removal of extracellular Ca2 + eliminates the spontaneous Ca^{2} oscillations, the removal of extracellular Ca^{2+}, L-type Ca^{2+} channel blockers, and N-methyl-D-aspartate receptor (NMDAR) or alpha-amino-3-hydroxy-5-methyl-4-isoxazolepropionic acid receptor (AMPAR) antagonists eliminates L-type Ca^{2+} channel blockers and oscillations[9–11].

[1]Department of Neurology, Graduate School of Medicine, Osaka University, Yamadaoka 2-2, Suita, Osaka 565-0871, Japan. [2]StemRIM Institute of Regeneration-Inducing Medicine, Osaka University, Yamadaoka 2-2, Suita, Osaka 565-0871, Japan. [3]Center for Supporting Drug Discovery and Life Science Research, Graduate School of Pharmaceutical Science, Osaka University, 1-6 Yamadaoka, Suita, Osaka 565-0871, Japan. [4]Graduate School of Comprehensive Rehabilitation, Osaka Prefecture University, Osaka 583-8555, Japan. ✉email: sasaki@neurol.med.osaka-u.ac.jp

The measurement of Ca^{2+} transients in rat cortical neurons by high-throughput fluorescence techniques would be of significant value in the assessment of seizure risk of compounds, particularly at the early stages of drug discovery. The 2D networks of primary cortical neurons have been employed in the assessment of potential neurotoxicity or epileptogenicity on multi-well microelectrode arrays[12–14] and Ca^{2+} oscillation assays, utilizing a microplate reader with Fluo-3/AM or Fluo-4 Ca^{2+} indicators[15,16]. The cultures of human induced pluripotent stem cell (iPSC)-derived neurons and astrocytes exhibit measurable spontaneous Ca^{2+} oscillations in both 2D cultures and 3D spheroids. The suitability of human iPSC-derived 3D cultures as biological substrates for the screening of modulators of spontaneous neuronal network activity was assessed. In the context of 2D and 3D hiPSC-derived neuronal networks, the parameters of frequency and amplitude of spontaneous global network Ca^{2+} oscillations and the directionality of drug-dependent Ca^{2+} oscillations have already been examined[17]. This study showed the impact of compound administration on Ca^{2+} oscillations in both 2D networks and 3D neurospheroids.

The Ca^{2+} oscillations were quantified in rat primary neurons using a camera-based kinetic plate reader, FDSS-7000, which enabled high-throughput analysis. The fluorescent dye, which is sensitive to calcium, was employed to this end. The FDSS-7000 is capable of simultaneous imaging of multiple samples (384–1536 wells) over time. This capability is made possible by the device's built-in batch aliquoter, which allows for reactions to be taken simultaneously in each well without a time lag. Furthermore, the FDSS-7000 assay system does not need specialized techniques or costly methodologies. It can be readily adapted as a medium- to high-throughput assay for the early detection of proarrhythmic and epileptogenic risk within the context of drug discovery and development[18]. We examined the effects of Library of Pharmacologically Active Compounds 1280 (LOPAC1280) compounds on Ca^{2+} oscillations and detected the drug-induced FDSS parameter changes on Ca^{2+} oscillations-waveforms.

The pathogenesis of cerebral ischemia is believed to be underpinned by glutamine toxicity induced by extracellular Ca^{2+}, which is thought to be a fundamental process underlying neuronal death[19,20]. One of the primary causes of glutamate excitotoxicity is the activation of the NMDAR subtype of glutamate receptor[21]. It has been demonstrated that NMDAR-dependent glutamate excitotoxicity can also be observed in human embryonic stem cell-derived neurons[22]. The study of NMDAR subtypes and localization has attracted significant attention due to the evidence that synaptic and extrasynaptic NMDARs exert distinct roles in excitotoxicity[23]. In particular, NR2A receptor subtypes are mainly located in synaptic NMDARs. On the other hand, NR2B subtypes are mainly located in extrasynaptic NMDARs. These subtypes have opposite effects on neuronal death or survival[24]. Furthermore, our findings indicate that Ro-256981, an NR2B-selective inhibitor, exerts neuroprotective effects following cerebral ischemia, whereas NVP-AAM0077, an NR2A-selective inhibitor, has the opposite effect[25,26]. The AMPA receptor subunit GluR2 also plays a role in determining the vulnerability of neurons in forebrain ischemia[27]. In summary, NMDA receptors play a pivotal role in the pathophysiology of cerebral ischemia. However, the precise way in which Ca^{2+} oscillations are modulated by selective inhibition of each subtype of NMDAR, specifically NR2A or NR2B, remains unclear.

Nicotinic acetylcholine receptors (nAChRs) are expressed at high levels in the central nervous system and play a pivotal role in regulating neural functions, including transmitter release, synaptic plasticity, brain circuits, and cognitive functions. Given the pivotal roles of glutamatergic and cholinergic neurotransmission in memory and learning, the regulation of cholinergic transmission is an attractive pharmacological therapeutic target for neurological disorders[28]. Preclinical studies targeting nAChRs have been conducted using animal models for various pathologies. A particularly promising approach is based on positive allosteric modulators (PAMs) of these receptors, which offer several advantages over direct agonists[29]. Nevertheless, few studies have examined the effects of nAChR subtypes and PAMs on Ca^{2+} oscillations within the neural network, focusing particularly on the PAM effect. The objective of this study was to compare the activity of type II PAM (PNU-120596), which potentiates agonist-evoked α7 nAChR currents, delays the desensitization process, and reactivates desensitized receptors, with type I PAM (NS-1738), which potentiates α7 nAChRs without modifying the desensitization process[1,30,31]. The objective of this study was to examine the impact of nAChR subtypes and PAMs on the frequency and amplitude of Ca^{2+} oscillations.

Despite the potential significance of spontaneous Ca^{2+} oscillations, there has been no comprehensive investigation into how Ca^{2+} oscillations are altered following ischemia. In this study, we sought to investigate the modulation of Ca^{2+} oscillations following in vitro ischemia or the treatment of nAChRs subtypes and PAMs using the kinetic plate reader system FDSS-7000. Ca^{2+} dysregulation contributes to neurodegeneration in iPSC-derived cells from patients with Friedreich's ataxia and Parkinson's disease[32,33]. Consequently, Ca^{2+} oscillation assays in neuronal cultures have considerable potential for modeling neurological diseases and toxicities, with applications in drug discovery and toxicology. The FDSS-7000 assay system may prove to be a valuable tool for the exploration of neuroprotective compounds against neurological disorders, including those associated with stroke.

Methods

Material

The following compounds were procured from Sigma-Aldrich (Burlington, MA, USA): MK-801, 4-AP, (-)-nicotine, and nifedipine. NS1738 and PNU282987 were procured from Cayman Chemical (Ann Arbor, MI, USA). Picrotoxin (PTX) and Gabazine were procured from Fujifilm (Chuo-Ku, Tokyo, Japan), while Dr. Yves Auberson of Novartis kindly provided NVP-AAM077. The following compounds were purchased from Tocris Bioscience (Wren Nest Rd, Glossop): CNQX, PNU-12059, RJR-2043, varenicline, and Ro25-6981.

Primary cortical cultures

The primary cultures of rat cortical neurons were obtained as described previously[26,34]. Carbon dioxide was employed as the euthanasia agent, while isoflurane was utilized as the anesthetic. In brief, neuronal cultures were prepared from the cortex of embryonic day 16 (E16) rat embryos (Charles River Laboratories Japan, Inc, Yokohama, Japan). The cells were dissociated with papain (Papain Dissociation System; Worthington) and plated at a density of 40,000 cells per well in a 384-well plate and incubated in 80 µl of high-glucose Dulbecco's Modified Eagle's Medium (DMEM) (Sigma) containing 10% fetal calf serum (FCS; Invitrogen), 100 IU/ml penicillin, and 100 µg/ml streptomycin sulfate. At 24 h after seeding, the medium was replaced with neurobasal plus medium (Invitrogen) supplemented with B-27 plus (Invitrogen). The cells were cultured at 37 °C in a humidified atmosphere of 95% air and 5% CO2 and used after 10–11 days in vitro, at which point most cells exhibited a neuronal phenotype. On the 14th day after plating, the cells were loaded with fluorescent EarlyTox dyes for Ca^{2+} transient measurements.

3D-spheroid culture

The neurons were cultivated on the 384-spheroid plates (Corning) or PrimeSurface plate 384U (Sumitomo Bakelite Co., Ltd., Tokyo, Japan) at a density of 40,000 cells per well.

Measurements of Ca^{2+} oscillation

The fluorescent dye used was EarlyTox Cardiotoxicity Kit (#R8211, Molecular Devices, LLC, San Jose, CA, USA) according to the manufacturer. It has previously been demonstrated that Ca^{2+} oscillations can be quantified using EarlyTox in both 2D and 3D culture systems of iPSC-derived neurons[35]. The EarlyTox Cardiotoxicity Kit utilizes a calcium-sensitive indicator equivalent to Cal520AM (#21131, AAT Bioquest, Sunnyvale, CA, USA) to detect intracellular Ca^{2+} concentrations. Indeed, Ca^{2+} oscillations have been previously quantified utilizing the FDSS-7000 in 384 wells with Cal520 dye[35]. Significant improvements in signal-to-noise ratio and cellular retention were observed in Cal-520 compared to Fluo-3 AM and Fluo-4 AM. Furthermore, it exhibits over 100 times greater fluorescence enhancement at longer wavelengths, rendering it highly suitable for measuring intracellular calcium[36–38]. Excitation and emission were performed at 485 nm and 535 nm, respectively. In comparison to Fura-2 and Fluo-4, Cal-520 exhibits superior sensitivity and brightness. Its quantum yield, when complexed with calcium, is 0.95, far exceeding the 0.3 observed of Fura-2, making Cal-520 particularly effective for detecting weak calcium signals[36]. Cal520 was maintained at 37 °C for the measurements of Ca^{2+} transients. Following the removal of the culture medium (60 µL), 20 µL of the dye solution was applied to the well (20 µL + 20 µL = total 40 µL) and incubated for 120 min at 37 °C in 5% CO2. The measurements were conducted for each medium. The 2D-culture system was evaluated at a Mg^{2+} concentration of 0.1 mM, while the 3D spheroid culture was assessed at a Mg^{2+} concentration of 1 mM. Following a single fluorescence measurement in the absence of test compounds (pre), 0.1% Dimethyl sulfoxide (DMSO) in culture medium was applied to the wells (40 µL + 5 µL), and the cells were incubated for 10 min at 37 °C in 5% CO2. Following the pretreatments, 5 µL of each test compound (10 × final concentration) in culture medium was applied to the wells (45 µL + 5 µL), and the cells were incubated for 10 min at 37 °C in 5% CO2. In this study, a library of pharmacologically active compounds (Office for University-Industry Collaboration, Osaka University, Japan) was utilized.

Fluorescence measurements and analysis

The fluorescence intensity changes in all wells of a microplate were recorded simultaneously at 37 °C using a kinetic plate reader, FDSS7000EX (Hamamatsu Photonics K.K., Shizuoka, Japan), with a sampling rate of 100 ms and a total of 6000 frames over 10-min.

The intracellular Ca^{2+} concentration changes (calcium waveforms) were analyzed using FDSS Waveform Analysis Software (Hamamatsu, Shizuoka, Japan), which estimated the peak rate (P rate (/min)), peak-to-peak time, peak width at 10–90%, rising slope, falling slope, and other parameters. All compounds were tested in a total of 5 to 21 samples. The results of each well were normalized with those of the control group (1.1% DMSO).

Oxygen glucose deprivation

Oxygen glucose deprivation (OGD) was conducted by placing the cultures in a 37 °C incubator housed in an anaerobic chamber, as previously described[26]. In this study, OGD was performed for 1, 2, and 3 h. For experiments involving drug loading after OGD, the medium was replaced with the respective drug-containing medium 5 min after OGD, and Ca^{2+} oscillation was measured 1 h later.

Statistical analysis

Most data are presented as mean ± standard deviation. A two-tailed, unpaired Student's t-test was employed to compare the means between the two groups. The Kruskal–Wallis test was used to compare more than three groups (Prism 10.0; GraphPad Software Inc., San Diego, CA, USA). If statistically significant differences were identified, Dunnett's T3 multiple comparison test was used for post-hoc analysis. The threshold for statistical significance was set at $P < 0.05$.

Study approval

The animal experimental protocol was approved by the Institutional Animal Care and Use Committee of Osaka University Graduate School of Medicine (Permission number: 30–091-001, 05–078-0000). All applicable international, national, and/or institutional guidelines for the care and use of animals were followed. Additionally, our study was in compliance with the ARRIVE guidelines.

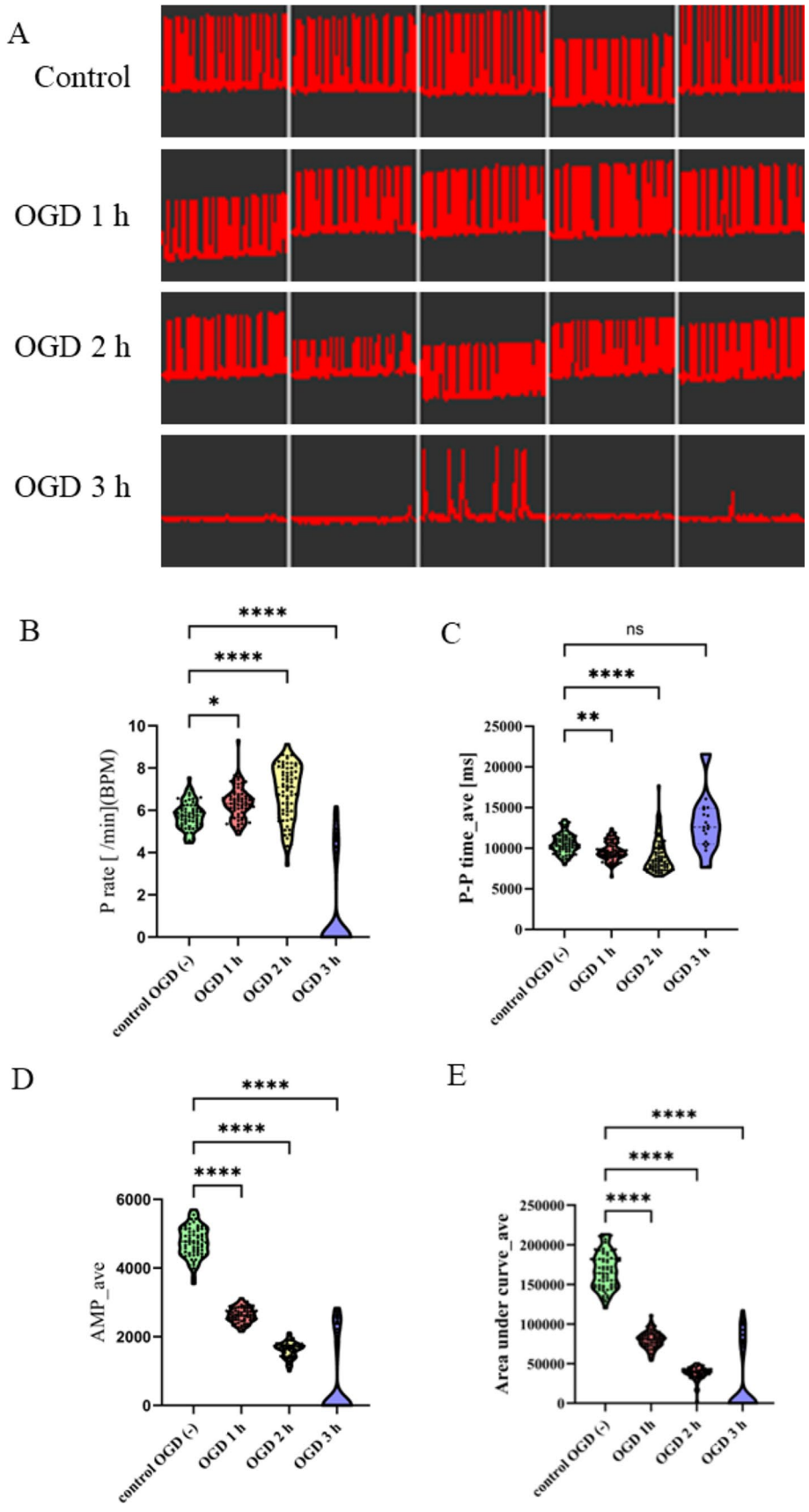

Results

Ca^{2+} oscillations in high-density neuronal cultures in a high-throughput screenable system (HTS)

Previously, it was reported that primary neurons from rats and mice develop spontaneous intracellular Ca^{2+}

◀**Fig. 1**. Ca^{2+} oscillations in response to in vitro ischemia, oxygen–glucose deprivation (OGD) in 2D networks in rat primary cortical neurons. (**A**) Ca^{2+} oscillations signal from without or with different OGD times wells in FDSS-7000 platform 60 min after application to the wells over a 10-min recording period. (n = 5 at each OGD time of 1, 2, and 3 h). Impact of 1, 2, and 3 h for OGD exposure on the Ca^{2+} oscillations frequency (P rate /min (BPM)) (**B**), P-P time (ms) (**C**), amplitude (**D**), and area under the curve using FDSS-7000 platform (n = 70 in control, n = 70 in 1 h-OGD, n = 70 in 2 h-OGD, n = 21 in 3 h-OGD wells per group). *p < 0.05, OGD vs. vehicle control, **p < 0.01, ****p < 0.001.

oscillations when cultured at high densities[11,16,39]. A study was conducted to determine the optimal number of primary rat neuronal cell culture systems per well to measure Ca^{2+} oscillations in HTS using the FDSS7000EX. The rat primary cultures were loaded with the fluorescence calcium indicator Cal520, which can be quantitatively assessed in real-time using FDSS7000EX.

In high-density cortical cultures (40,000 cells per well in 384-well plates), we observed spontaneous Ca^{2+} oscillations developing around 2–3 weeks of incubation when observed in real-time in 2D systems (Supp. Video 1). Therefore, we decided to work with cultures at 2 weeks in vitro and 40,000 cells per well for all subsequent pharmacological studies. The oscillation patterns of Ca^{2+} were analyzed using a variety of quantifiable readouts, including peak count, average peak amplitude, average peak spacing, average peak width, and average rise and decay times (Supplementary Fig. 1).

In vitro, ischemia modulates Ca^{2+} oscillations in 2D systems

The impact of varying the duration of exposure to OGD, an in vitro ischemia, from 1 to 2 and 3 h on Ca^{2+} oscillations was investigated (Fig. 1A). First, the frequency of firing was examined by peak rate, burst per minute (BPM) (Fig. 1B), Peak-to-Peak time (P-P time) (Fig. 1C), amplitude (Fig. 1D), and area under the curve (AUC) (Fig. 1E). OGD at 1 and 2 h significantly increased the frequency of excitation, while the 3-h OGD resulted in a significant reduction in firing (Fig. 1B–C). The amplitude of the response decreased in a time-dependent manner following exposure to OGD (Fig. 1D). The AUC also demonstrated a time-dependent decrease in response to OGD (Fig. 1E). The RMP, rising slope, and falling slope also exhibited a decrease in proportion to the duration of OGD (Supplementary Fig. 1).

Pretreatment of compounds controls the activity of voltage- and ligand-gated ion channels and can control Ca^{2+} oscillations

We investigated the effects of those compounds on Ca^{2+} oscillations in the control condition without OGD before examining the effects of various compounds on the modulation of ischemia-potentiating Ca^{2+} oscillations (Supplementary Fig. 2). The influence of 4-aminopyridine (4-AP), a voltage-dependent K + channel (KV) blocker, on Ca^{2+} dynamics in cortical neurons was studied (Supplementary Fig. 2). These compounds have been identified as having epileptogenic properties in Ca^{2+} oscillations. The frequency of spontaneous Ca^{2+} oscillations was significantly increased in 4-AP (Supplementary Fig. 2).

Subsequently, the impact of various compounds on the modulation of Ca^{2+} oscillations following in vitro ischemia (OGD) was examined. Consequently, we elected to administer the compounds in advance of the 2-h OGD for all subsequent pharmacological studies (Fig. 2). The influence of 4-AP, PTX, and gabazine on Ca^{2+} dynamics in cortical neurons was studied, revealing an increased frequency of spontaneous Ca^{2+} oscillations following 2 h of OGD in 4-AP, but not in PTX and gabazine (Fig. 2B–D).

The subsequent investigation sought to ascertain the potential involvement of NMDARs and AMPARs in the observed effects on Ca^{2+} oscillations under control conditions and following ischemic conditions. Similar to the findings of a previous report, the pretreatment of MK-801 resulted in a notable reduction in frequency at a concentration of 0.3 uM and the cessation of Ca^{2+} oscillation at higher concentrations (Supplementary Fig. 3A)[39]. NVP-AAM0077, an NMDA NR2A subunit blocker, demonstrated a concentration-dependent increase in the frequency of Ca^{2+} oscillations, accompanied by a significant increase in amplitude (Supplementary Fig. 3B) (Fig. 3A). Conversely, Ro256981, an NMDA NR2B subunit blocker, demonstrated a concentration-dependent reduction in the frequency of Ca^{2+} oscillations (Supplementary Fig. 3C).

NVP-AAM0077 exhibited a slight influence on the frequency and amplitude of Ca^{2+} oscillations (Fig. 3B). The frequency of Ca^{2+} oscillations was suppressed at high concentrations (5 uM) by Ro256981, and a concentration-dependent reduction in the frequency of Ca^{2+} oscillations was observed (Fig. 3C). The results demonstrated that Ro256981 exhibited a similar trend to that of MK-801, although MK-801 exhibited a more pronounced effect than Ro256981. Preincubation of CNQX, a potent and competitive AMPA/kainate receptor antagonist, resulted in a concentration-dependent reduction in the frequency of Ca^{2+} oscillations. Conversely, CNQX exhibited a concentration-dependent increase in the amplitude of Ca^{2+} oscillations (Fig. 3D).

Ca^{2+} oscillations in 3D-spheroid high-density cortical culture

The next step was to examine the spontaneous Ca^{2+} oscillations in 3D-spheroid cultures of neurons. In high-density cortical cultures (40,000 cells per well in 384-well plates), we also observed spontaneous $Ca2^{+}$ oscillations in real-time in 3D spheroid systems (Supplementary Video 2). For baseline readings, without compound addition, the coefficient of variation for peak count was observed across a representative 384-well plate (data not shown), indicating consistent performance between different wells. The oscillatory activity of neurons exposed to the vehicle remained stable throughout the entire recording period (Fig. 4 A,B). 4-AP (5–500 µM) was found to elicit a concentration-dependent increase in spontaneous Ca^{2+} oscillations, with no significant effect on the amplitude of Ca^{2+} oscillations (Figs. 4C and 5A). The concentration-dependent suppression of the frequency

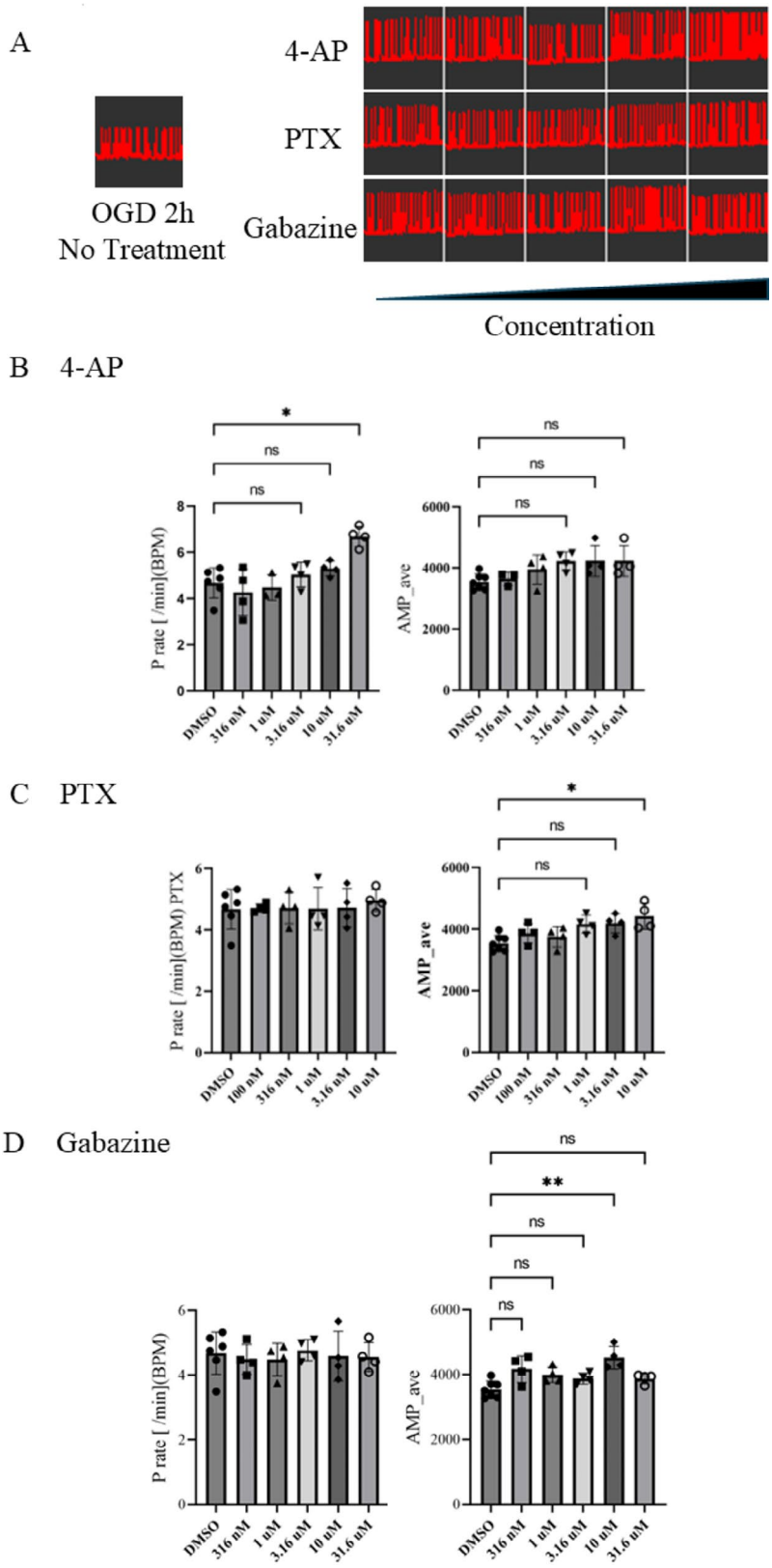

Fig. 2. 4-AP, PTX, and gabazine partially augment ischemia-induced activation of Ca^{2+} oscillations in 2D networks in rat primary cortical neurons. (**A**) Representative images illustrating the effect of pre-exposure to 4-Aminopyridine (0.1 μM), PTX, (0.1 μM) or a gabazine (0.1 μM) on ischemia-induced Ca^{2+} oscillations modulation. Effect of 4-AP (B), PTX, (**C**), or gabazine (**D**) pre-treatment on OGD-induced increase in transient frequency and amplitude in Ca^{2+} oscillations. *$p < 0.05$, OGD plus compounds vs. vehicle control, $n = 5$ pooled from two experiments.

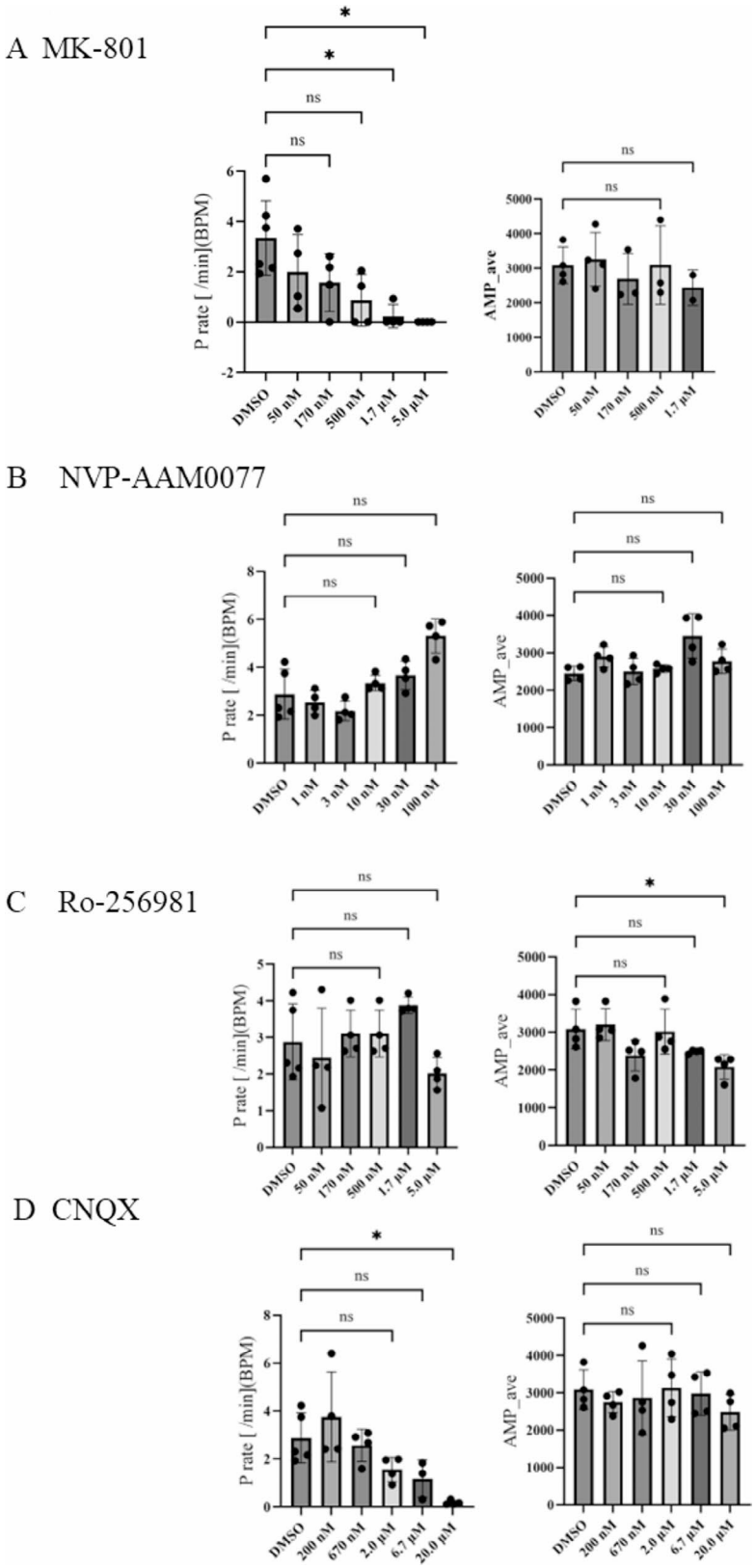

Fig. 3. NMDA receptor compounds partially mitigate ischemia-induced activation of Ca^{2+} oscillations in 2D networks in rat primary cortical neurons. The effect of pretreatment of 4-AP (**A**), MK-801, an NMDA receptor blocker (1 μM) (**B**), NVP-AAM0077, a relatively selective NMDA NR2A receptor blocker (1 μM) (**C**), Ro-256981, a selective NMDA NR2B receptor blocker (1 μM) (**D**), or CNQX, an AMPA receptor blocker (1 μM) on OGD-induced increase of transient frequency and amplitude in Ca^{2+} oscillations. *$p < 0.05$, OGD plus compounds vs. vehicle control, $n = 5$ pooled from two experiments.

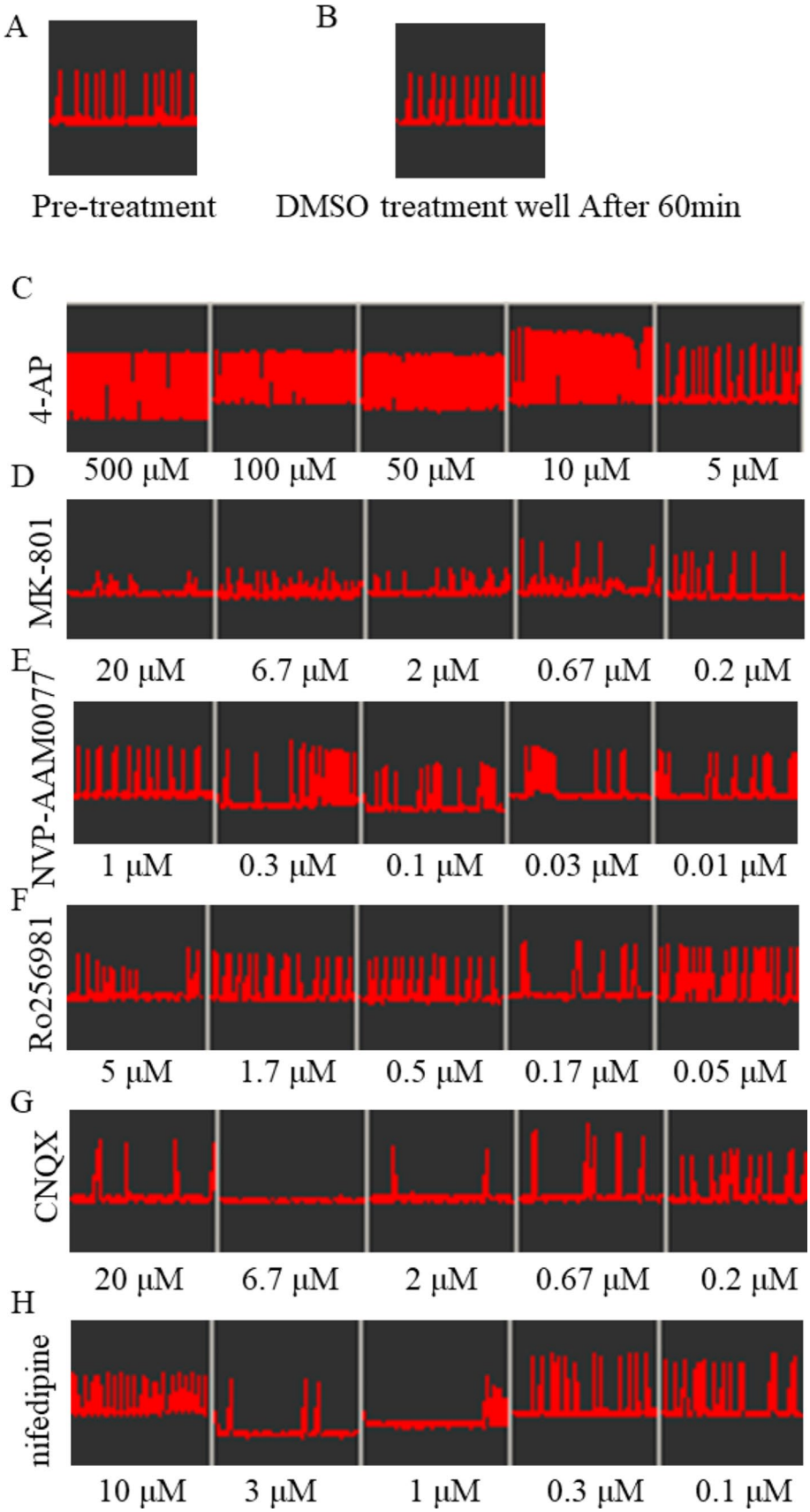

and amplitude of Ca^{2+} oscillations (Figs. 4D and 5B) were observed following the administration of MK-801 (200 nM–20 μM). The administration of NVP-AAM0077 had no significant effect on the frequency or amplitude of Ca^{2+} oscillations within the range measured. However, there was a tendency for the frequency of Ca^{2+} oscillations to increase at higher concentrations (100 nM), although this was not statistically significant (Figs.

◀**Fig. 4**. Representative images showing how acute exposure to compounds influences Ca^{2+} oscillations in 3D neuro-spheroids of cortical neurons. Ca^{2+} oscillations from pretreatment (**A**) or vehicle (0.1% DMSO) (**B**) wells 60 min after application to the wells over a 10-min recording period. (n = 12 neuro-spheroids at each condition). (**C**) 4-AP was applied to 3D neuro-spheroids at concentrations of 5 uM up to 500 µM with the signal recorded for 10 min. Each concentration was applied to five adjacent spheroids and incubated for 60 min before reading Ca^{2+} activity in the FDSS platform. (**D**) MK-801 concentrations were applied to 3D neuro-spheroids at concentrations of 0.2 uM up to 20 µM. (**E**) NVP-AAM0077 concentrations were applied to 3D neuro-spheroids at concentrations of 0.01 uM up to 1 µM. (**F**) Ro-256981 concentrations were applied to 3D neuro-spheroids at concentrations of 0.05 uM up to 5 µM. (**G**) CNQX concentrations were applied to 3D neuro-spheroids at concentrations of 0.2 uM up to 20 µM. (**H**) Nifedipine concentrations were applied to 3D neuro-spheroids at concentrations of 0.1 uM up to 10 µM. n = 5 neuro-spheroids at each condition.

4E and 5C). The administration of Ro-256981 resulted in a reduction in the frequency and amplitude of Ca^{2+} oscillations, with the effect on amplitude reaching statistical significance at a concentration of 5 µM (Figs. 4F and 5D). The introduction of CNQX (2.0, 6.7, or 2 µM) resulted in a reduction in the frequency of spontaneous Ca^{2+} oscillation (Figs. 4G and 5E). The concentration-dependent suppression of the frequency of Ca^{2+} oscillations was observed in the presence of nifedipine (100 nM–3 µM), with the effect on amplitude reaching significance at 3 µM (Figs. 4H and 5F). Nifedipine also caused a partial activation of the frequency of Ca^{2+} oscillations without any significance, as previously reported.

Nicotinic α7 receptors facilitate the firing of Ca^{2+} oscillations

Subsequently, we investigated the impact of nicotine signaling on Ca^{2+} oscillations. Nicotine significantly increased the frequency of Ca^{2+} oscillations at high concentrations (Supplementary Fig. 4). Given the high expression of α7 and α4β2 nicotinic receptors in the central nervous system, agonists for each receptor were administered to examine their differing effects on Ca^{2+} oscillation. PNU-282987, an α7nAChR agonist, was observed to elicit a concentration-dependent increase in the frequency of Ca^{2+} oscillations (Fig. 6A). In contrast, neither of the α4β2 agonists, RJR-2043 and varenicline, demonstrated this effect (Fig. 6B,C). The compounds did not affect the amplitude of the Ca^{2+} oscillations (Fig. 6A–C).

The impact of α7-nAChR PAMs, namely NS-1738 (type 1 PAM) and PNU-120596 (type 2 PAM), on Ca^{2+} oscillations in cortical neurons was examined. The combination of nicotine and PNU-120596 significantly increased the frequency of Ca^{2+} oscillations in a concentration-dependent manner, even at relatively low concentrations of nicotine (10 µM) (Fig. 7A). Similarly to PNU-120596, the combination of NS-1738 and nicotine also resulted in a significant increase in the firing frequency of Ca^{2+} oscillations. Moreover, NS-1738 was found to significantly increase the amplitude of Ca^{2+} oscillations in a concentration-dependent manner (Fig. 7B). NS-1738 also augmented the frequency of Ca^{2+} oscillations when combined with PNU-272987 (Fig. 7C).

Discussion

The measurement of Ca^{2+} transients in rat cortical neurons by high-throughput fluorescence techniques would be of significant value in the assessment of seizure risk of compounds, particularly at the early stages of drug discovery. This study also demonstrated that Ca^{2+} oscillations were modified by in vitro ischemia, which could be used to screen neuroprotective drugs for stroke. Furthermore, our findings indicate that Ca^{2+} oscillations exhibit differential responses to distinct nAChR subtypes and are influenced by PAMs of nAChRs.

The results of this study demonstrate the utility of this assay in high-throughput screening and provide an innovative approach for CNS-based drug discovery in both 2D and 3D systems. It is crucial to differentiate between beneficial therapeutic effects and potential epilepsy-inducing neuronal toxicity[35]. In the field of new drug development, new approach methods (NAMs) that combine organoids, tissue chips, and in silico studies without animal testing are attracting attention. The Food and Drug Administration (FDA) Modernization Act 2.0 will be important in evaluating these methods in a way that connects in vitro and in vivo mouse models in the future[40,41].

It is well established that during the initial period of in vitro cultivation, there is minimal network activity. However, Ca^{2+} oscillations can be observed during this process. Following 7–10 days in vitro, spontaneous Ca^{2+} oscillations are observed in every neuron within the region of interest. Moreover, the density of synapses and frequency of oscillatory activity increase in mature cultures after 14 days in vitro[9]. The measurements of Ca^{2+} oscillations in our culture system are also in close agreement with the results mentioned above. As network activity is the result of a multitude of interconnected processes, including structural interactions, cell health, neuronal firing, synaptic transmission, and a plethora of additional cellular processes, it is evident that a comprehensive understanding of the underlying mechanisms is essential. Ca^{2+} oscillations can serve as a global phenotypic readout for both normal and pathophysiological functions[42]. The 3D system is more physiologically relevant than the 2D system, as the two cell types exist in a more natural state. This increased physiological relevance may be advantageous in the screening of novel compounds that modulate neuronal network activity[42]. The 3D sphere platform may provide a phenotypic approach to interrogating neurological diseases, with the potential to lead to the development of therapies. The microBrain 3D neurospheres have also been employed to profile neurotoxic compounds, thereby demonstrating the extensive applicability of this platform[43].

Conversely, it has been demonstrated that 2D culture systems can detect epileptogenicity with greater efficacy than 3D models[35]. In this study, we performed in vitro ischemia (OGD) in a 2D model. Further investigation is necessary to determine whether hypoxic conditions may result in heterogeneous penetration of hypoxia into the more central regions of the sphere in the 3D culture.

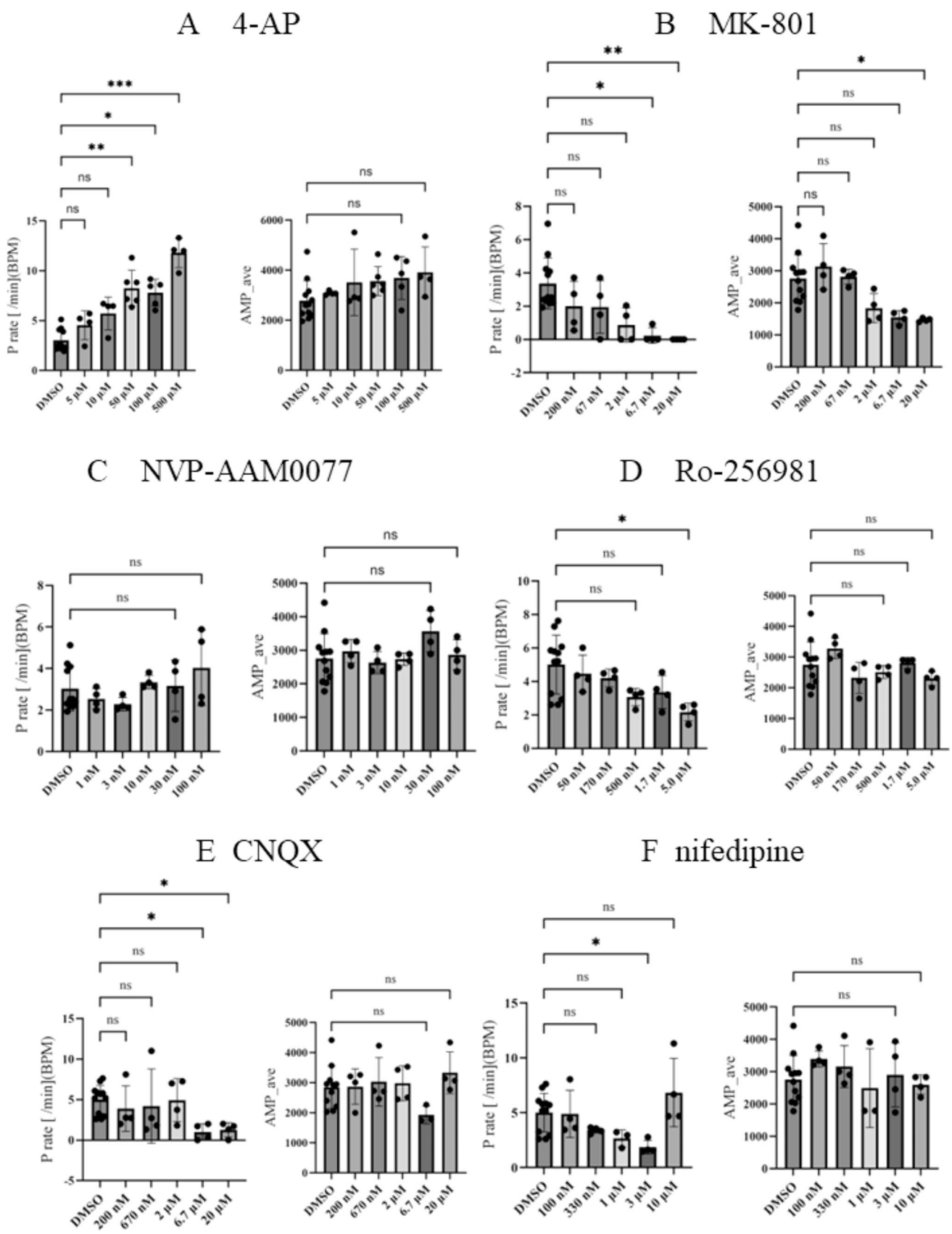

The Ca^{2+} oscillation assay shows promise in improving prediction accuracy in early drug development. Wang et al. used a 3D neurospheroid model derived from human iPS cells to assess the neurotoxicity of 84 drugs using this assay. The compounds were divided into two sets: a central nervous system target set (58 drugs) and a test set (26 drugs), which included well-established clinical compounds. Neurotoxicity scores from a logistic regression model, demonstrated 93% specificity and 53% sensitivity, effectively differentiating

◀**Fig. 5**. The effect of compounds on spontaneous Ca^{2+} oscillations. Bar graph shows the effect of 4-AP treatment on the frequency and amplitude 60 min after application to the wells. (**B**) Bar graph shows the effect of MK-801 treatment on the frequency and amplitude 60 min after application to the wells. (**C**) Bar graph shows the effect of NVP-AAM0077 treatment on the frequency and amplitude 60 min after application to the wells. (**D**) Bar graph shows the effect of Ro-256981 treatment on the frequency and amplitude 60 min after application to the wells. (**E**) Bar graph shows the effect of CNQX treatment on the frequency and amplitude 60 min after application to the wells. (**F**) Bar graph shows the effect of nifedipine treatment on the frequency and amplitude 60 min after application to the wells. Compared with the control condition, $^{*}P < 0.05$, $^{**}P < 0.01$. n = 5 neuro-spheroids at each condition.

neurotoxic from non-neurotoxic compounds, with a low false positive rate for predicting seizures, convulsions, and neurodegeneration[44]. Moreover, the use of spheroids on specific brain regions has reproduces neurological disease progression and facilitated drug screening, such as in Alzheimer's disease and opioid use disorder models[45]. Additionally, a report evaluated the effects of ten potential proarrhythmic compounds on Ca^{2+} oscillations using five human iPSC-derived cardiomyocyte lines in a 384-well plate system to, detecting changes in Ca^{2+} oscillation duration across all cell lines. This HTS approach demonstrates its potential for a assessing proarrhythmic risk[46]. These studies highlight the Ca^{2+} oscillation assay's utility in improving prediction accuracy in early drug development.

A relatively brief OGD of 1 or 2 h increased the firing frequency of Ca^{2+} oscillations while simultaneously reducing their amplitude in a time-dependent manner (Fig. 1). Given that MK-801, CNQX, and nifedipine suppressed Ca^{2+} oscillations under physiological conditions, Ca^{2+} influx through NMDA receptors, AMPA receptors, and VGCCs is of significant importance. Furthermore, OGD-enhanced increases in Ca^{2+} oscillation frequency were also suppressed by NMDA and AMPA receptors (Fig. 3). This aligns with previous findings that repeated short-term hypoxia regulates calcium responses of ionotropic glutamate receptors in hippocampal neurons[47]. NR2B-mediated NMDAR influx may be particularly significant (Fig. 3). Additionally, after the two-hour OGD, KV inhibition further increased Ca^{2+} oscillation frequency, whereas GABAA receptor inhibition by picrotoxin and gabazine did not (Fig. 2B–D). These findings indicate that two hours of OGD impairs GAGAA receptor signaling in Ca^{2+} oscillations. This posthypoxic hyperexcitability, caused by synchronous Ca^{2+} spiking in network-forming neurons during reoxygenation[47–49], has been linked to Ca^{2+}-dependent selective death of certain GABAergic neurons[49]. These findings suggest that short-term OGD-induced increases in Ca^{2+} oscillation frequency result from a decrease in GABAA receptor signaling. The reduction in the amplitude of Ca^{2+} oscillations can be attributed to a decline in the number of synchronising neurons and a general diminution in the Ca^{2+} response resulting from OGD.

Rising and FallingSlope parameters showed a significant decline in OGD time dependence (Supplementary Fig. 1), reflecting potential changes in Ca^{2+} kinetics after OGD, warranting further investigation. Conversely, prolonged OGD (> 3 h) has been demonstrated to cause excessive calcium influx through glutamate receptors, contributing to mitochondrial dysfunction and neuronal damage[26,50]. The cessation of Ca^{2+} oscillations observed in this study after 3 h of OGD likely results from this mechanism.

The concentrations of compounds affecting Ca^{2+} oscillations were determined based on findings from previous studies in primary rat neurons, including MEA (microelectrode array) assays. Compounds such as 4-AP, PTZ, gabazine, MK-801, CNQX, nifedipine, NVP-AAM0077, Ro-256981, nicotine, PNU282987, RJR-2403, and PNU120596 have been used in previous studies[9,16,25,26,39,51–55]. These compounds were investigated for their impact on Ca^{2+} oscillations in both primary rat neuron cultures and iPSCs[35,56]. The concentrations used in these studies derived from prior research, particularly focusing on neuroprotective effects and electrophysiological responses. Furthermore, the concentrations used in this study were determined by referencing those tested in in vivo animal studies, and other relevant sources, including the reports described by Wang et al.[44].

A variety of in vitro assays using neuronal cells or brain tissue from animal origin have also been deemed applicable to detect drug-induced seizure liabilities[57–59]. However, it is well documented that there may be species-specific differences in sensitivity to drug-induced seizures among various preclinical animals, and there may also be some differences when compared to the outcome in humans[60–62]. hiPSC-derived neurons co-cultured in 3D spheroids have been proposed as a promising model for phenotypic in vitro profiling and potential use[42,44,63]. Nevertheless, in vitro assays utilizing hiPSC-derived neurons and/or astrocytes, and in vivo animal models are expensive and inefficient with relatively low throughput. Given the low cost and ease of production of primary mouse and rat neuronal cultures, the application of a combination of these approaches could increase throughput and reduce concerns about species differences between preclinical assays and outcomes in humans[35].

Two complementary methods have been employed to assess neuronal function. The techniques employed were calcium imaging and multi-electrode array (MEA). The MEA can be employed to identify, in real-time, quantal excitatory or inhibitory transmission occurring from numerous neurons within a network. In contrast to MEA, which records the action potential spikes of cell bodies at the surface of the network and infers concerted network activity via temporal spike correlation analysis, Ca^{2+} oscillations provide a direct measure of the integrated activity of cell bodies, as well as dendritic and synaptic activity, which are not accessible to the planar MEA electrode. The time course of stabilization of Ca^{2+} spike activity across the network has been demonstrated to follow a predictable timeline when isolated neurons are plated in multi-well screening plates, which are commonly used in standard Ca^{2+} fluorescent reader platforms[16,64]. MEA electrodes are very expensive, and the number of electrodes that can be recorded per well is limited.

Furthermore, the utilization of Ca^{2+}-sensitive fluorescent dyes enables the implementation of an intermediate to high-throughput assay that is not significantly reliant on the technical expertise of the technician, in contrast

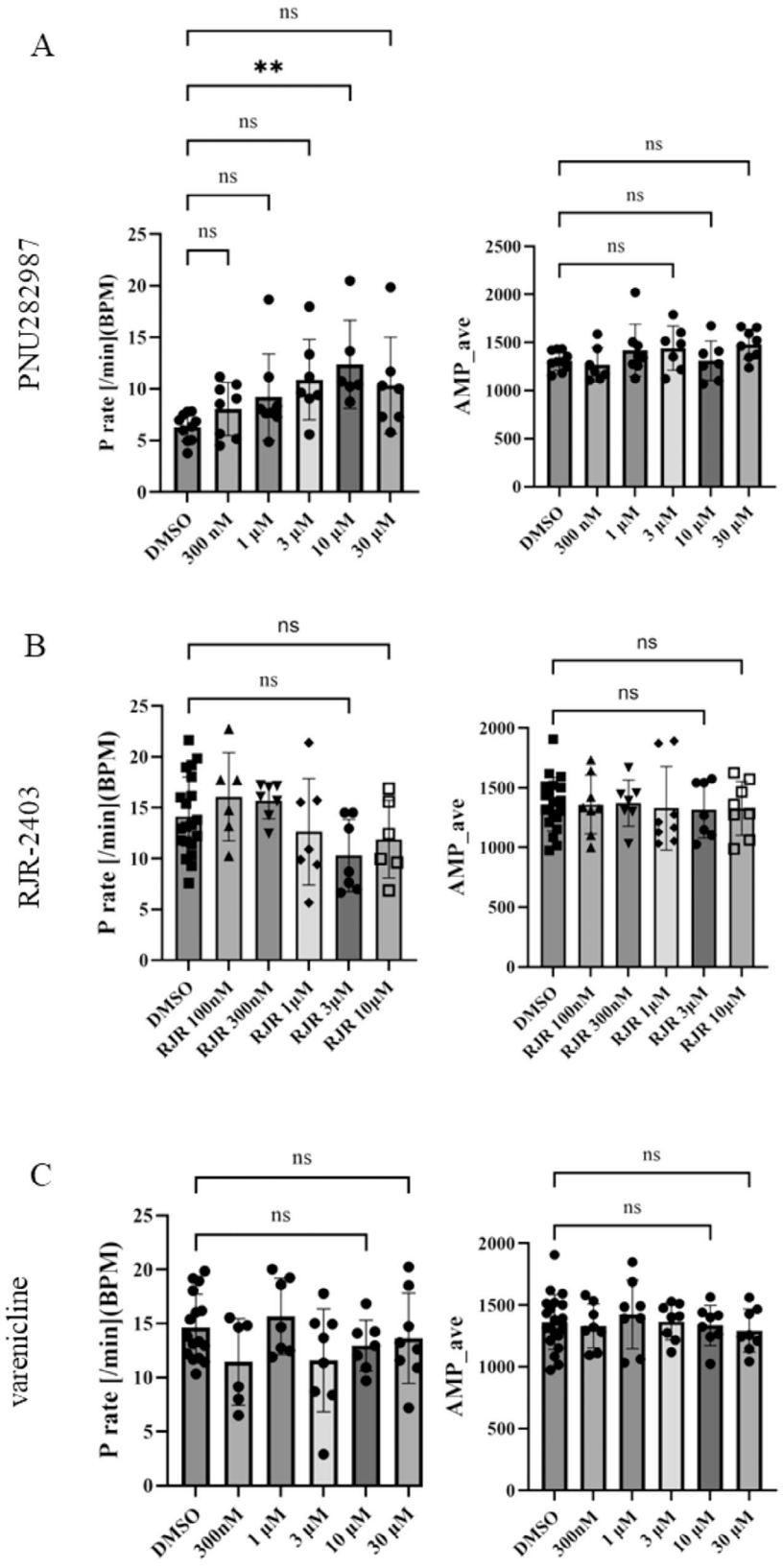

Fig. 6. α7 nAChRs and α4β2 modulate Ca^{2+} oscillations. (**A**) PNU-282987, an α7nAChR agonist, concentrations were applied to 3D neuro-spheroids at concentrations of 0.3 uM up to 30 µM. (**B**) RJR-4023, α4β2 agonists, concentrations were applied to 3D neuro-spheroids at concentrations of 0.1 uM up to 10 µM. (**C**) α4β2 agonists varenicline concentrations were applied to 3D neuro-spheroids at concentrations of 0.05 uM up to 5 µM. Compared with the DMSO control condition, $^{*}P < 0.05$, $^{**}P < 0.01$. n = 8 neuro-spheroids at each condition.

to other electrophysiological recordings such as manual patch clamp or MEA. The MEA technology has been utilized in in vitro assays with hiPSC neurons. Yet, its relatively low throughput represents a limitation of this approach in the early phase of drug development[12]. Conversely, Ca^{2+} transient imaging using calcium-sensitive fluorescent dyes has been employed for in vitro screening at a considerably higher throughput. In this approach, Ca^{2+} transients exhibited waveforms of synchronized neuronal Ca^{2+} oscillations. The morphology and frequency of these phenomena may be readily detected as modulators of neuronal receptors and ion channels[15,65–67]. Ca^{2+} oscillation has also been extensively employed in the early detection of proarrhythmic and cardiogenic risk in the discovery and development of new drugs. This investigation indicates that the Ca^{2+} transient assay can serve as a reliable alternative to the other two assay systems (MEA and voltage-sensing optical (VSO) recording)[35]. The integrative nature of the Ca^{2+} signal also allows for clear interpretation of network signals, regardless of whether they originate from 2D- or 3D-cellular networks. The reason is that global parameters, such as network Ca^{2+} spiking frequencies and amplitudes, can be readily compared between models.

Ca^{2+} influx from extracellular sources with or without Ca^{2+} mobilization from intracellular stores is important for Ca^{2+} oscillations[9]. The influx of Ca^{2+} via L-type calcium channels appears to be required, while the influence of N-, T-, P, or Q-type channels on the frequency of Ca2 + oscillations is evident, yet not absolute[9]. The inhibition of voltage-gated K channels by TEA and 4-AP also induces Ca^{2+} oscillations; however, this is independent of NMDA receptor activation since 4-AP-induced Ca^{2+} oscillations cannot be inhibited by either Mg^{2+} or MK-801. However, AMPA receptors appear to be required as CNQX suppressed Ca^{2+} oscillations under all conditions examined[9]. We found that MK-801 and CNQX completely suppressed Ca oscillations enhanced by ischemia (OGD) in a concentration-dependent manner. These observations indicate that Ca^{2+} oscillations observed in control conditions and those enhanced by ischemia may be the result of combining shared and distinct mechanisms. Both excitotoxicity in ischemia and Ca^{2+} oscillations are inhibited by the pan-NMDA receptor antagonist MK-801, indicating that intracellular Ca^{2+} influx through both NMDA receptors is crucial. Synaptic NMDARs, which are predominantly NR2A receptor subtypes, and extrasynaptic NMDARs, which are mainly NR2B subtypes, have opposite effects on neuronal death or survival[24]. The objective of this study was to ascertain whether the inhibition of either NR2A or NR2B of the NMDA receptors had different effects on Ca^{2+} oscillations. In control conditions, the inhibition of NR2A and NR2B had opposing effects on the frequency of Ca^{2+} oscillations. The inhibition of NR2A increases the frequency of Ca^{2+} oscillations, whereas the inhibition of NR2B decreases it. In contrast, no significant difference was observed in the frequency of Ca^{2+} oscillations following OGD. Further investigation is required to determine the optimal duration of ischemia, subtype selectivity, and concentration of NMDA inhibitors. A novel drug, Nelonemdaz, which acts as an NR2B inhibitor in the treatment of acute cerebral infarction, is still under investigation[68].

Nifedipine exhibited a concentration-dependent effect on Ca^{2+} oscillations, with a significant decrease in frequency observed at concentrations below 3 uM and an increase in frequency at higher concentrations (10 uM) (Fig. 5F). Nifedipine has been demonstrated to elicit a sustained facilitation of tetrodotoxin-insensitive spontaneous glutamate release independent of its L-type calcium channel blocking effect[69]. Nifedipine acts on the release process downstream of Ca^{2+} entry or release[69]. The glutamate-releasing effect of nifedipine was also confirmed in this system.

The targeting of α7 nAChRs and PAMs represents a promising approach to the treatment of neurological diseases, including stroke and neurodegenerative disorders[70–73]. Although there are numerous subtypes of nicotine receptors, α7 and α4β2 are predominantly expressed in the central nervous system[28]. Agonists of α7 nAChRs were observed to increase the frequency of Ca^{2+} oscillations, whereas agonists of α4β2 nAChRs did not elicit a similar response. Both α4β2- and α7-nAChRs have been demonstrated to mediate nicotine-induced Ca^{2+} oscillations through distinct regulatory mechanisms in primary cortical neurons. The co-administration of α7 nAChRs and α4β2 antagonists has been shown to completely prevent nicotine-induced increases in the firing frequency and amplitude of Ca^{2+} oscillations[74]. Nevertheless, the density of neuronal cultures in the study mentioned above was considerably lower than that in our assay system. Such differences in conditions may have resulted in different outcomes.

We tested whether both type I (do not modify desensitization) and type II (delay desensitization) PAMs could control Ca^{2+} oscillations and whether there were differences between them. PNU-120596, a type 2 PAM, acts via the activation of α7 nAChRs, resulting in increased channel conductance and permeability due to increased channel opening time. In contrast, NS1738, a type I PAM, has no such effect[29]. The type II PAM PNU-120596 has been reported to demonstrate significant anti-edematous and anti-allodynic effects in models of inflammatory and pain[75]. PNU-120596 has been demonstrated to reduce cerebral infarct volume in a rat model of middle cerebral artery occlusion, both when administered before and after the onset of the ischemic event[76]. PNU-120596 with PAM inhibits α7 desensitization and leads to sustained α7 activation, which may maximize its neuroprotective effect[76–78]. The desensitization state of α7 nAChRs induced by NS-6740, an α7 nAChR partial agonist, was sensitive to PNU-120596, as evidenced by the ability of PNU-120596 to reactivate α7 nAChRs desensitized by NS-6740. This ability to reactivate α7 nAChRs resulted in robust α7 nAChR-mediated currents. The re-activation of α7 nAChRs desensitized by NS-6740 resulted in the generation of robust α7 nAChR-mediated currents, thereby enabling the observation of NS-6740-induced α7 nAChR-mediated currents[79,80]. The co-administration of nicotine with PNU-120596 was found to increase the frequency of Ca^{2+} oscillations, consistent with the findings observed in human iPS-derived neurons[56]. PNU-282987 (10 μM) exhibited no efficacy when administered alone; however, when combined with PNU-120596 (3 μM), intracellular Ca^{2+} levels were significantly enhanced in a concentration-dependent manner[56]. Both intermediate type-I/II PAMs (JNJ-39393406, AF58801) and type-II PAMs (PNU-120596, TQS) demonstrated a concentration-dependent increase in intracellular Ca^{2+}, which could be inhibited by MLA[56]. The results obtained are in accordance with those previously reported for human iPS-derived neurons, thereby indicating that the FDSS-7000 assay system for Ca^{2+} oscillation is a valuable tool in the search for neuroprotective compounds.

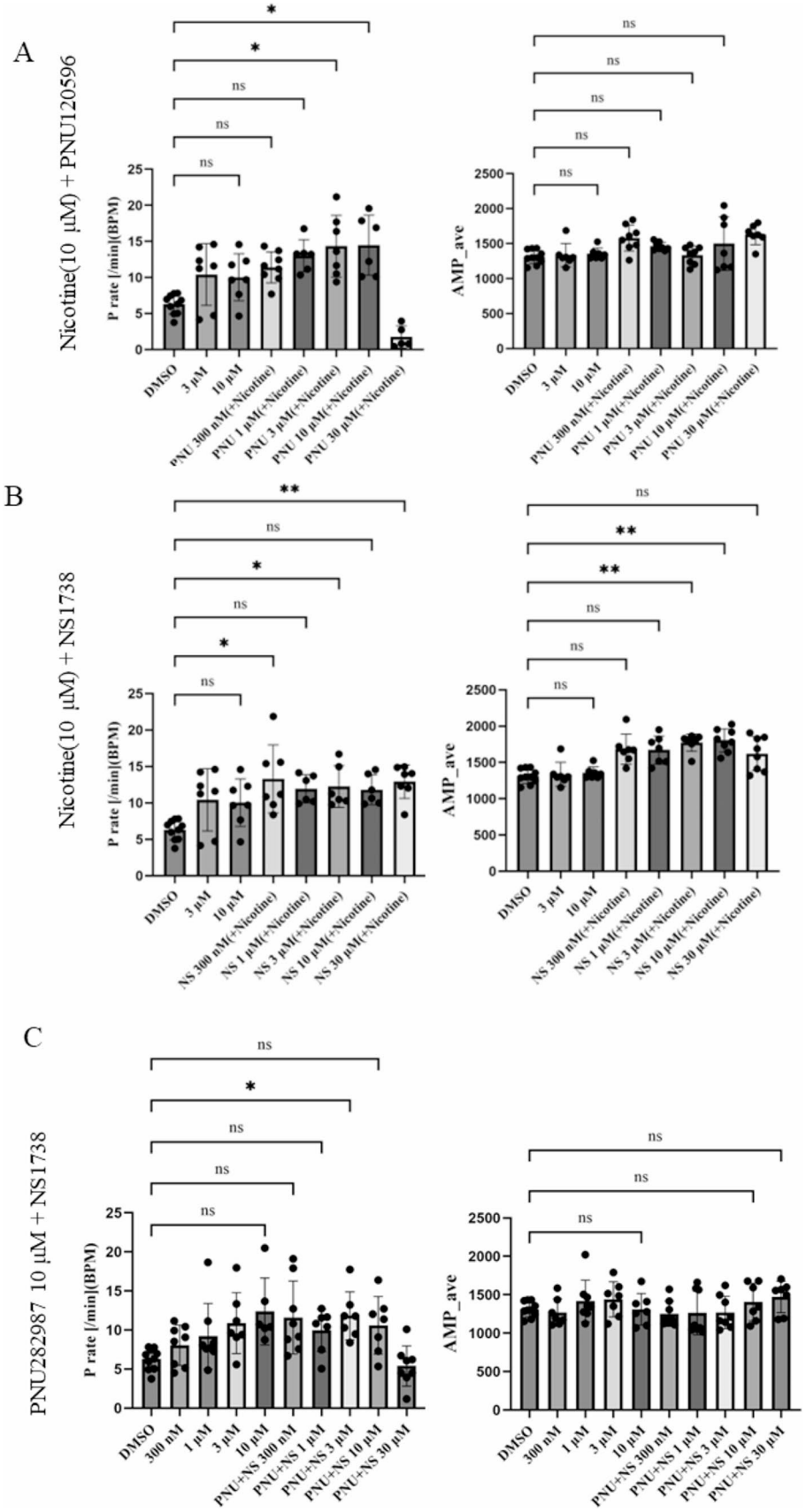

A comparison between data obtained from standard fluorescence microscopy and high-throughput screening methods highlights several differences. First, there is a reduction in spatial resolution[81]. While FDSS or FLIPR are highly effective for detecting Ca^{2+} signals in high-throughput screening, they offer lower spatial resolution compared to microscopes, making it difficult to observe intricate calcium dynamics within neurons or individual

◀**Fig. 7**. Control of Ca^{2+} oscillations by type I (do not modify desensitization) and type II PAMs and differences in response between them. (**A**) Nicotine (10 uM) plus type II PAM PNU-120596 concentrations were applied to 3D neuro-spheroids at concentrations of 0.3 uM up to 30 μM. Concentration-dependent activation of type II PAM PNU-120596 in the presence of nicotine (10 uM). (**B**) Nicotine (10 uM) plus type I PAM NS-1738 concentrations were applied to 3D neuro-spheroids at concentrations of 0.3 uM up to 30 μM. (**C**) PNU-272987 plus type I PAM NS-1738 concentrations were applied to 3D neuro-spheroids at concentrations of 0.3 uM up to 30 μM. Compared with the DMSO control condition, $^{*}P < 0.05$, $^{**}P < 0.01$. n = 8 neuro-spheroids at each condition.

synaptic changes. Microscopy, particularly two-photon microscopy, capture precise calcium fluctuations within individual nerve processes and synapses[82]. Second, temporal resolution is constrained in FLIPR and FDSS[81]. While they rapidly screen Ca^{2+} responses across cell populations, they miss the detailed kinetics of Ca^{2+} oscillations that require higher temporal resolutions[83]. Third, the HTS system using FDSS or FLIPR focuses on cellular responses at the population level, averaging Ca^{2+} oscillation data across cells. This limits the ability to assess the specific functions of individual neurons and synapses, as the results are influenced by the most active neurons. In contrast, microscopy provides detailed insights into intracellular Ca^{2+} fluctuations and changes in synaptic structure and function. Lastly, image size is a limitation with microscopy. The large, complex images generated require manual processing of the region of interest (ROI) for target cells showing Ca^{2+} oscillatory behavior, making data analysis time-consuming and challenging to manage.

In conclusion, microscopy offers greater precision for Ca^{2+} oscillation kinetics, whereas HTS systems like FLIPR/FDSS are better suited for large-scale, rapid screening with lower temporal and spatial resolutions. Microscopy is preferred for detailed kinetic studies, whereas HTS excels in high-throughput drug screening. Additionally, the FDSS method offers advantages over traditional animal-based toxicity tests, enabling simultaneous testing of multiple compounds in numerous wells. Although FDSS lacks data on cortical structures found in slice cultures, as they are derived from dissociated cells.

This study had several limitations. First, the relatively small number of compounds tested necessitates further studies with more drugs, particularly those with seizure risk or neuroprotective compounds, to validate the results. Another limitation lies in the methodology employed by FDSS in conducting the assay. The FDSS-7000 provides integrated single data on cell activity, dendrites, and synaptic activity in real time. For more detailed insights, researchers may consider high content screening (HCS) technology, such as kinetic image cytometry[84]. The MEA can be utilized to identify, in real-time, quantal excitatory or inhibitory transmission occurring from numerous neurons within a network[55,85], and assess a multitude of parameters, including the electric efficiency between neighboring neurons. However, careful interpretation is needed when analyzing the results, especially when a compound exerts conflicting effects on Ca^{2+} oscillations between neurons and astrocytes. The assay's comprehensive design within a single well has inherent limitations. In primary cultures where neurons are predominant, even a small number of astrocytes with opposing reactions can influence the overall direction of Ca^{2+} oscillation, which ultimately reflects the net effect of neuronal input: either excitatory or inhibitory. Neurons typically exhibit a low baseline firing rate, allowing only the rising portion of the signal to be detected. Unlike neurons, astrocytes do not generate action potentials; however, they can regulate neurotransmission through calcium signaling[86]. Furthermore, MEA/FDSS has been proven effective in evaluating epileptogenicity using primary rat neuronal cultures. A seizure risk prediction model based on 113 reference drugs demonstrated high overall accuracy (92.78%), with strong sensitivity and specificity[55]. Although sensitivity was lower for neuroactive compounds, the model still maintained high specificity and accuracy (81.82%)[55]. Further investigation is required to ascertain the suitability of in vitro ischemia (OGD) conditions for high-throughput assays in Ca^{2+} oscillations using FDSS-7000. The prolonged incubation periods with Ca^{2+} dyes have been demonstrated to influence cell physiology, including the inhibition of Na^{+}/K^{+}-ATPase or cytoskeletal disassembly[87].

Preclinical studies of neuroprotective agents in stroke using cellular and animal models have not yielded satisfactory results in human clinical trials. In this study, we investigated the dynamics of Ca^{2+} oscillations following ischemia at a high-throughput level and elucidated the effects of nicotinic compounds on Ca^{2+} oscillations in the 3D space. Ca^{2+} oscillation is regarded as a pivotal assay method, including the utilization of animal-free induced pluripotent stem cells (iPSCs) and organoids or as a functional assay. In the search for new drugs for stroke, Ca^{2+} oscillation appears to be a useful approach in neuronal cultures and culture systems combining various cells.

Data availability

The authors declare that all data supporting the findings of this study are available in the paper, as well as its Supplementary Information.

Received: 27 July 2024; Accepted: 25 October 2024
Published online: 12 November 2024

References

1. Andersen, N. D. et al. Exploring the positive allosteric modulation of human alpha7 nicotinic receptors from a single-channel perspective. *Neuropharmacology* **107**, 189–200 (2016).
2. Berridge, M. J. Neuronal calcium signaling. *Neuron* **21**, 13–26 (1998).
3. Miller, R. J. The control of neuronal Ca2+ homeostasis. *Prog Neurobiol* **37**, 255–285 (1991).
4. Berridge, M. J. Elementary and global aspects of calcium signalling. *J Exp Biol* **200**, 315–319 (1997).

5. Dravid, S. M. & Murray, T. F. Spontaneous synchronized calcium oscillations in neocortical neurons in the presence of physiological [Mg(2+)]: involvement of AMPA/kainate and metabotropic glutamate receptors. *Brain Res* **1006**, 8–17 (2004).
6. Cohen, S. & Greenberg, M. E. Communication between the synapse and the nucleus in neuronal development, plasticity, and disease. *Annu Rev Cell Dev Biol* **24**, 183–209 (2008).
7. Kuijlaars, J. et al. Sustained synchronized neuronal network activity in a human astrocyte co-culture system. *Sci Rep* **6**, 36529 (2016).
8. Ichikawa, M., Muramoto, K., Kobayashi, K., Kawahara, M. & Kuroda, Y. Formation and maturation of synapses in primary cultures of rat cerebral cortical cells: an electron microscopic study. *Neurosci Res* **16**, 95–103 (1993).
9. Wang, X. & Gruenstein, E. I. Mechanism of synchronized Ca2+ oscillations in cortical neurons. *Brain Res* **767**, 239–249 (1997).
10. Shimizu, M., Nishida, A. & Yamawaki, S. Antidepressants inhibit spontaneous oscillations of intracellular Ca2+ concentration in rat cortical cultured neurons. *Neurosci Lett* **146**, 101–104 (1992).
11. Robinson, H. P. et al. Periodic synchronized bursting and intracellular calcium transients elicited by low magnesium in cultured cortical neurons. *J Neurophysiol* **70**, 1606–1616 (1993).
12. Bradley, J. A., Luithardt, H. H., Metea, M. R. & Strock, C. J. In vitro screening for seizure liability using microelectrode array technology. *Toxicol Sci* **163**, 240–253 (2018).
13. Strickland, J. D., Martin, M. T., Richard, A. M., Houck, K. A. & Shafer, T. J. Screening the ToxCast phase II libraries for alterations in network function using cortical neurons grown on multi-well microelectrode array (mwMEA) plates. *Arch Toxicol* **92**, 487–500 (2018).
14. Tukker, A. M., Wijnolts, F. M. J., de Groot, A. & Westerink, R. H. S. Applicability of hiPSC-derived neuronal cocultures and rodent primary cortical cultures for in vitro seizure liability assessment. *Toxicol Sci* **178**, 71–87 (2020).
15. Hemstapat, K., Smith, M. T. & Monteith, G. R. Measurement of intracellular Ca2+ in cultured rat embryonic hippocampal neurons using a fluorescence microplate reader: potential application to biomolecular screening. *J Pharmacol Toxicol Methods* **49**, 81–87 (2004).
16. Pacico, N. & Mingorance-Le Meur, A. New in vitro phenotypic assay for epilepsy: Fluorescent measurement of synchronized neuronal calcium oscillations. *PLoS ONE* **9**, e84755 (2014).
17. Imredy, J. P., Roussignol, G., Clouse, H., Salvagiotto, G. & Mazelin-Winum, L. Comparative assessment of Ca(2+) oscillations in 2- and 3-dimensional hiPSC derived and isolated cortical neuronal networks. *J Pharmacol Toxicol Methods* **123**, 107281 (2023).
18. Lu, H. R. et al. Assessing drug-induced long QT and proarrhythmic risk using human stem-cell-derived cardiomyocytes in a Ca2+ imaging assay: Evaluation of 28 CiPA compounds at three test sites. *Toxicol Sci* **170**, 345–356 (2019).
19. Hahn, J. S., Aizenman, E. & Lipton, S. A. Central mammalian neurons normally resistant to glutamate toxicity are made sensitive by elevated extracellular Ca2+: toxicity is blocked by the N-methyl-D-aspartate antagonist MK-801. *Proc Natl Acad Sci USA* **85**, 6556–6560 (1988).
20. Mody, I. & MacDonald, J. F. NMDA receptor-dependent excitotoxicity: the role of intracellular Ca2+ release. *Trends Pharmacol Sci* **16**, 356–359 (1995).
21. Lipton, S. A. Paradigm shift in neuroprotection by NMDA receptor blockade: memantine and beyond. *Nat Rev Drug Discov* **5**, 160–170 (2006).
22. Gupta, K., Hardingham, G. E. & Chandran, S. NMDA receptor-dependent glutamate excitotoxicity in human embryonic stem cell-derived neurons. *Neurosci Lett* **543**, 95–100 (2013).
23. Sattler, R., Xiong, Z., Lu, W. Y., MacDonald, J. F. & Tymianski, M. Distinct roles of synaptic and extrasynaptic NMDA receptors in excitotoxicity. *J Neurosci* **20**, 22–33 (2000).
24. Hardingham, G. E., Fukunaga, Y. & Bading, H. Extrasynaptic NMDARs oppose synaptic NMDARs by triggering CREB shut-off and cell death pathways. *Nat Neurosci* **5**, 405–414 (2002).
25. Terasaki, Y. et al. Activation of NR2A receptors induces ischemic tolerance through CREB signaling. *J Cereb Blood Flow Metab* **30**, 1441–1449 (2010).
26. Sasaki, T. et al. SIK2 is a key regulator for neuronal survival after ischemia via TORC1-CREB. *Neuron* **69**, 106–119 (2011).
27. Peng, P. L. et al. ADAR2-dependent RNA editing of AMPA receptor subunit GluR2 determines vulnerability of neurons in forebrain ischemia. *Neuron* **49**, 719–733 (2006).
28. Fowler, C. D., Arends, M. A. & Kenny, P. J. Subtypes of nicotinic acetylcholine receptors in nicotine reward, dependence, and withdrawal: evidence from genetically modified mice. *Behav Pharmacol* **19**, 461–484 (2008).
29. Hurst, R. S. et al. A novel positive allosteric modulator of the alpha7 neuronal nicotinic acetylcholine receptor: in vitro and in vivo characterization. *J Neurosci* **25**, 4396–4405 (2005).
30. Arias, H. R. et al. Novel positive allosteric modulators of the human alpha7 nicotinic acetylcholine receptor. *Biochemistry* **50**, 5263–5278 (2011).
31. Targowska-Duda, K. M., Feuerbach, D., Biala, G., Jozwiak, K. & Arias, H. R. Antidepressant activity in mice elicited by 3-furan-2-yl-N-p-tolyl-acrylamide, a positive allosteric modulator of the alpha7 nicotinic acetylcholine receptor. *Neurosci Lett* **569**, 126–130 (2014).
32. Imamura, K. et al. Calcium dysregulation contributes to neurodegeneration in FTLD patient iPSC-derived neurons. *Sci Rep* **6**, 34904 (2016).
33. Eglen, R. M. & Reisine, T. Human iPS cell-derived patient tissues and 3D cell culture part 2: Spheroids, organoids, and disease modeling. *SLAS Technol* **24**, 18–27 (2019).
34. Goldberg, M. P. & Choi, D. W. Combined oxygen and glucose deprivation in cortical cell culture: Calcium-dependent and calcium-independent mechanisms of neuronal injury. *J Neurosci* **13**, 3510–3524 (1993).
35. Lu, H. R., *et al.* High-throughput screening assay for detecting drug-induced changes in synchronized neuronal oscillations and potential seizure risk based on ca(2+) fluorescence measurements in human induced pluripotent stem cell (hiPSC)-derived neuronal 2D and 3D cultures. *Cells* **12**(2023).
36. Tada, M., Takeuchi, A., Hashizume, M., Kitamura, K. & Kano, M. A highly sensitive fluorescent indicator dye for calcium imaging of neural activity in vitro and in vivo. *Eur J Neurosci* **39**, 1720–1728 (2014).
37. Lock, J. T., Parker, I. & Smith, I. F. A comparison of fluorescent Ca(2)(+) indicators for imaging local Ca(2)(+) signals in cultured cells. *Cell Calcium* **58**, 638–648 (2015).
38. Bergmann, G. A. & Bicker, G. Cholinergic calcium responses in cultured antennal lobe neurons of the migratory locust. *Sci Rep* **11**, 10018 (2021).
39. Cao, Z. et al. Tetramethylenedisulfotetramine alters Ca(2)(+) dynamics in cultured hippocampal neurons: mitigation by NMDA receptor blockade and GABA(A) receptor-positive modulation. *Toxicol Sci* **130**, 362–372 (2012).
40. Moutinho, S. Researchers and regulators plan for a future without lab animals. *Nat Med* **29**, 2151–2154 (2023).
41. Han, J. J. FDA Modernization Act 2.0 allows for alternatives to animal testing. *Artif Organs* **47**, 449–450 (2023).
42. Woodruff, G. et al. Screening for modulators of neural network activity in 3D human iPSC-derived cortical spheroids. *PLoS ONE* **15**, e0240991 (2020).
43. Sirenko, O. et al. Functional and mechanistic neurotoxicity profiling using human iPSC-derived neural 3D cultures. *Toxicol Sci* **167**, 58–76 (2019).
44. Wang, Q. et al. Assessment of a 3D neural spheroid model to detect pharmaceutical-induced neurotoxicity. *ALTEX* **39**, 560–582 (2022).

45. Strong, C. E. et al. Functional brain region-specific neural spheroids for modeling neurological diseases and therapeutics screening. *Commun Biol* **6**, 1211 (2023).
46. Wakatsuki, T. et al. Bayesian approach enabled objective comparison of multiple human iPSC-derived Cardiomyocytes' Proarrhythmia sensitivities. *J Pharmacol Toxicol Methods* **128**, 107531 (2024).
47. Turovskaya, M. V. et al. Repeated brief episodes of hypoxia modulate the calcium responses of ionotropic glutamate receptors in hippocampal neurons. *Neurosci Lett* **496**, 11–14 (2011).
48. Godukhin, O., Savin, A., Kalemenev, S. & Levin, S. Neuronal hyperexcitability induced by repeated brief episodes of hypoxia in rat hippocampal slices: involvement of ionotropic glutamate receptors and L-type Ca(2+) channels. *Neuropharmacology* **42**, 459–466 (2002).
49. Turovsky, E. A., Turovskaya, M. V., Kononov, A. V. & Zinchenko, V. P. Short-term episodes of hypoxia induce posthypoxic hyperexcitability and selective death of GABAergic hippocampal neurons. *Exp Neurol* **250**, 1–7 (2013).
50. Bickler, P. E., Fahlman, C. S. & Ferriero, D. M. Hypoxia increases calcium flux through cortical neuron glutamate receptors via protein kinase C. *J Neurochem* **88**, 878–884 (2004).
51. Hu, M. et al. High content screen microscopy analysis of A beta 1–42-induced neurite outgrowth reduction in rat primary cortical neurons: neuroprotective effects of alpha 7 neuronal nicotinic acetylcholine receptor ligands. *Brain Res* **1151**, 227–235 (2007).
52. Yang, K. et al. Distinctive nicotinic acetylcholine receptor functional phenotypes of rat ventral tegmental area dopaminergic neurons. *J Physiol* **587**, 345–361 (2009).
53. Di Cesare Mannelli, L., Tenci, B., Zanardelli, M., Failli, P. & Ghelardini, C. alpha7 nicotinic receptor promotes the neuroprotective functions of astrocytes against oxaliplatin neurotoxicity. *Neural Plast* **2015**, 396908 (2015).
54. Fan, J. et al. Assessing seizure liability using multi-electrode arrays (MEA). *Toxicol In Vitro* **55**, 93–100 (2019).
55. Kreir, M. et al. Development of a new hazard scoring system in primary neuronal cell cultures for drug-induced acute neuronal toxicity identification in early drug discovery. *Front Pharmacol* **15**, 1308547 (2024).
56. Larsen, H. M., Hansen, S. K., Mikkelsen, J. D., Hyttel, P. & Stummann, T. C. Alpha7 nicotinic acetylcholine receptors and neural network synaptic transmission in human induced pluripotent stem cell-derived neurons. *Stem Cell Res* **41**, 101642 (2019).
57. Kreir, M. et al. Do in vitro assays in rat primary neurons predict drug-induced seizure liability in humans?. *Toxicol Appl Pharmacol* **346**, 45–57 (2018).
58. Tukker, A. M. & Westerink, R. H. S. Novel test strategies for in vitro seizure liability assessment. *Expert Opin Drug Metab Toxicol* **17**, 923–936 (2021).
59. Avoli, M. & Jefferys, J. G. Models of drug-induced epileptiform synchronization in vitro. *J Neurosci Methods* **260**, 26–32 (2016).
60. DaSilva, J. K. et al. Nonclinical species sensitivity to convulsions: An IQ DruSafe consortium working group initiative. *J Pharmacol Toxicol Methods* **103**, 106683 (2020).
61. Zhai, J., Zhou, Y. Y. & Lagrutta, A. Sensitivity, specificity and limitation of in vitro hippocampal slice and neuron-based assays for assessment of drug-induced seizure liability. *Toxicol Appl Pharmacol* **430**, 115725 (2021).
62. Larson, E. A., Accardi, M. V., Zhong, Y., Paquette, D. & Authier, S. Drug-induced seizures: Considerations for underlying molecular mechanisms. *Int J Toxicol* **40**, 403–412 (2021).
63. Hogberg, H. T. & Smirnova, L. The future of 3D brain cultures in developmental neurotoxicity testing. *Front Toxicol* **4**, 808620 (2022).
64. Richards, G. R., Jack, A. D., Platts, A. & Simpson, P. B. Measurement and analysis of calcium signaling in heterogeneous cell cultures. *Methods Enzymol* **414**, 335–347 (2006).
65. Sirenko, O., Hesley, J., Rusyn, I. & Cromwell, E. F. High-content high-throughput assays for characterizing the viability and morphology of human iPSC-derived neuronal cultures. *Assay Drug Dev Technol* **12**, 536–547 (2014).
66. Leybaert, L. & Sanderson, M. J. Intercellular Ca(2+) waves: mechanisms and function. *Physiol Rev* **92**, 1359–1392 (2012).
67. Fu, M. et al. Deoxyschisandrin modulates synchronized Ca2+ oscillations and spontaneous synaptic transmission of cultured hippocampal neurons. *Acta Pharmacol Sin* **29**, 891–898 (2008).
68. Hong, J. M. et al. Nelonemdaz for patients with acute ischemic stroke undergoing endovascular reperfusion therapy: A randomized phase II trial. *Stroke* **53**, 3250–3259 (2022).
69. Hirasawa, M. & Pittman, Q. J. Nifedipine facilitates neurotransmitter release independently of calcium channels. *Proc Natl Acad Sci USA* **100**, 6139–6144 (2003).
70. Gaidhani, N., Tucci, F. C., Kem, W. R., Beaton, G. & Uteshev, V. V. Therapeutic efficacy of alpha7 ligands after acute ischaemic stroke is linked to conductive states of alpha7 nicotinic ACh receptors. *Br J Pharmacol* **178**, 1684–1704 (2021).
71. Sun, F., Jin, K. & Uteshev, V. V. A type-II positive allosteric modulator of alpha7 nAChRs reduces brain injury and improves neurological function after focal cerebral ischemia in rats. *PLoS ONE* **8**, e73581 (2013).
72. Dineley, K. T. et al. Beta-amyloid activates the mitogen-activated protein kinase cascade via hippocampal alpha7 nicotinic acetylcholine receptors: In vitro and in vivo mechanisms related to Alzheimer's disease. *J Neurosci* **21**, 4125–4133 (2001).
73. O'Neill, M. J., Murray, T. K., Lakics, V., Visanji, N. P. & Duty, S. The role of neuronal nicotinic acetylcholine receptors in acute and chronic neurodegeneration. *Curr Drug Targets CNS Neurol Disord* **1**, 399–411 (2002).
74. Wang, J. et al. Nicotinic modulation of Ca2+ oscillations in rat cortical neurons in vitro. *Am J Physiol Cell Physiol* **310**, C748-754 (2016).
75. Freitas, K., Ghosh, S., Ivy Carroll, F., Lichtman, A. H. & Imad Damaj, M. Effects of alpha7 positive allosteric modulators in murine inflammatory and chronic neuropathic pain models. *Neuropharmacology* **65**, 156–164 (2013).
76. Kalappa, B. I., Sun, F., Johnson, S. R., Jin, K. & Uteshev, V. V. A positive allosteric modulator of alpha7 nAChRs augments neuroprotective effects of endogenous nicotinic agonists in cerebral ischaemia. *Br J Pharmacol* **169**, 1862–1878 (2013).
77. Gusev, A. G. & Uteshev, V. V. Physiological concentrations of choline activate native alpha7-containing nicotinic acetylcholine receptors in the presence of PNU-120596 [1-(5-chloro-2,4-dimethoxyphenyl)-3-(5-methylisoxazol-3-yl)-urea]. *J Pharmacol Exp Ther* **332**, 588–598 (2010).
78. Callahan, P. M., Hutchings, E. J., Kille, N. J., Chapman, J. M. & Terry, A. V. Jr. Positive allosteric modulator of alpha7 nicotinic-acetylcholine receptors, PNU-120596 augments the effects of donepezil on learning and memory in aged rodents and non-human primates. *Neuropharmacology* **67**, 201–212 (2013).
79. Chojnacka, K., Papke, R. L. & Horenstein, N. A. Synthesis and evaluation of a conditionally-silent agonist for the alpha7 nicotinic acetylcholine receptor. *Bioorg Med Chem Lett* **23**, 4145–4149 (2013).
80. Papke, R. L., Peng, C., Kumar, A. & Stokes, C. NS6740, an alpha7 nicotinic acetylcholine receptor silent agonist, disrupts hippocampal synaptic plasticity. *Neurosci Lett* **677**, 6–13 (2018).
81. Sharma, P., Ando, D. M., Daub, A., Kaye, J. A. & Finkbeiner, S. High-throughput screening in primary neurons. *Methods Enzymol* **506**, 331–360 (2012).
82. Kalb, J., Nielsen, T., Fricke, M., Egelhaaf, M. & Kurtz, R. In vivo two-photon laser-scanning microscopy of Ca2+ dynamics in visual motion-sensitive neurons. *Biochem Biophys Res Commun* **316**, 341–347 (2004).
83. Weisenburger, S., *et al.* Volumetric Ca(2+) Imaging in the Mouse Brain Using Hybrid Multiplexed Sculpted Light Microscopy. *Cell* **177**, 1050–1066 e1014 (2019).
84. Cerignoli, F. et al. High throughput measurement of Ca(2)(+) dynamics for drug risk assessment in human stem cell-derived cardiomyocytes by kinetic image cytometry. *J Pharmacol Toxicol Methods* **66**, 246–256 (2012).
85. Odawara, A., Matsuda, N., Ishibashi, Y., Yokoi, R. & Suzuki, I. Toxicological evaluation of convulsant and anticonvulsant drugs in human induced pluripotent stem cell-derived cortical neuronal networks using an MEA system. *Sci Rep* **8**, 10416 (2018).

86. Koizumi, S. Synchronization of Ca2+ oscillations: involvement of ATP release in astrocytes. *FEBS J* **277**, 286–292 (2010).
87. Bootman, M. D., Allman, S., Rietdorf, K. & Bultynck, G. Deleterious effects of calcium indicators within cells; an inconvenient truth. *Cell Calcium* **73**, 82–87 (2018).

Author contributions
TS, SH, KN and BL planned the study. TS, SH, HK, KN, BL, KN, SM, and TK performed the experiments. TS and SH wrote the manuscript. TS, SH, HK, TK, KT, SM, and HM reviewed and revised the manuscript. All authors read and approved the manuscript.

Funding
This work was supported by the following grants: JSPS KAKENHI Grant number 21K07414 (to T.S.) and Smoking Research Foundation (to T.S.)

Declarations

Competing interests
The authors declare no competing interests.

Ethics approval
All experiments were performed following the Use of Laboratory Animals and ARRIVE guidelines. The Institutional Animal Care and Use Committee of Osaka University Graduate School of Medicine approved all animal protocols and experiments (Permission number: 30-091-001, 05-078-0000).

Consent for publication
All authors give their consent and approval for publication of this manuscript.

Additional information
Supplementary Information The online version contains supplementary material available at https://doi.org/10.1038/s41598-024-77882-w.

Correspondence and requests for materials should be addressed to T.S.

Reprints and permissions information is available at www.nature.com/reprints.

Publisher's note Springer Nature remains neutral with regard to jurisdictional claims in published maps and institutional affiliations.